e-ISSN: 2582-5208
International Research Journal of Modernization in Engineering Technology and Science
Volume:02/Issue:09/September-2020 Impact Factor- 5.354 www.irjmets.com

PREDICTION OF MEASURED POWER SPECTRAL DENSITY OF GSM 900 REVERSE LINK USING ARTIFICIAL NEURAL NETWORK

Frederick Ojiemhende Ehiagwina*1, Eze Blessing Ebere*2

*1Department of Electrical/Electronic Engineering, Federal Polytechnic Offa, Offa, Kwara State, Nigeria.

*2Department of Computer Engineering, Federal Polytechnic Ilaro, Ogun State, Nigeria.

ABSTRACT

An efficient spectrum resource utilization demands continuous spectrum sensing, this however is costly. Spectrum prediction has been proposed as a solution to continuous spectrum sensing. By conception, spectrum prediction utilizes previous spectrum measurements to forecasts the future status of the channel. In this paper, Artificial Neural Network (ANN) is explored in the prediction of spectrum occupancy of 925 - 960 MHz link in a selected location in Ilorin, Nigeria. Different sample partitions were examined. The sample partition 70-15-15% of training, validation and testing gave the best Mean Square Error of 3.9090 for the predicted power spectral densities based on frequency points and MSE of 0.0025 for the predicted power spectral densities based on time instances.

Keywords: ANN, artificial neural network, cognitive radio network, spectrum occupancy, spectrum prediction.

I. INTRODUCTION

Continuous spectrum measurement is not only financially burdensome but also time-consuming. This has motivated the deployment of prediction techniques and algorithms to spectrum data. By conception, spectrum prediction utilizes previous spectrum measurements to forecasts future states of channel, whether vacant or occupied (Xing et al. 2013a, Yang & Zhao, 2015). Studies like that of Tumuluru et al. (2010) have shown that when spectrum prediction techniques are applied to spectrum management; there are merits. Firstly, there is an increased in the bandwidth utilized owing to an anticipated low probability of error in the forecast of vacant channels. Secondly, since the bandwidth can be predicted for the next time slot, the data rates may be adapted with the available bandwidth in view.

Researches such as those of Tumuluru et al. (2010), Bai et al. (2015), Zhang et al. (2019), Hou et al. (2017) and Supraja & Pitchai (2019) have applied various architecture of neural network in the prediction of future spectrum states. Others techniques used include Markov model (Li et al. 2010, Zhao et al. 2016), Bayesian inference (Jacob et al. 2014, Xing et al. 2013b), static-neighbour-graph (Bütün et al. 2010), Duty Cycle modelling (Bepari et al. 2019) and time series models such as ARIMA, Holt-Winter, etc. (Wang & Salous, 2011, Su & Wu, 2009, Safari, 2017).

Artificial Neural Network (ANN) seeks to mimic the Biological Neural Network (BNN). Whereas a BNN is made up of biological neurons, physically connected in the nervous system, the ANN consists of artificial neurons functionally interconnected, creating a programme-like structure with the capacity to mimic the behaviour and processes of biological neurons in terms of organization and learning. Thus, ANN possesses some features of the brain like massive parallelism, adaptivity, ability to learn and generalize, distributed representation and computation. Other features include the ability to process contextual information, low energy consumption, and fault tolerance.

Neural network-based techniques are preferable to for example Markov based prediction models, because in Markov models, knowing the optimal number of states is not easy, and more so it requires a complex computational process. More so, Markov models require large memory storage for keeping bulky past observations and continuous training of the predictive system. Owing to the rapid adaption required of cognitive radio, ANN has been used to predict the future actions of the PU.

e-ISSN: 2582-5208
International Research Journal of Modernization in Engineering Technology and Science
Volume:02/Issue:09/September-2020 Impact Factor- 5.354 www.irjmets.com

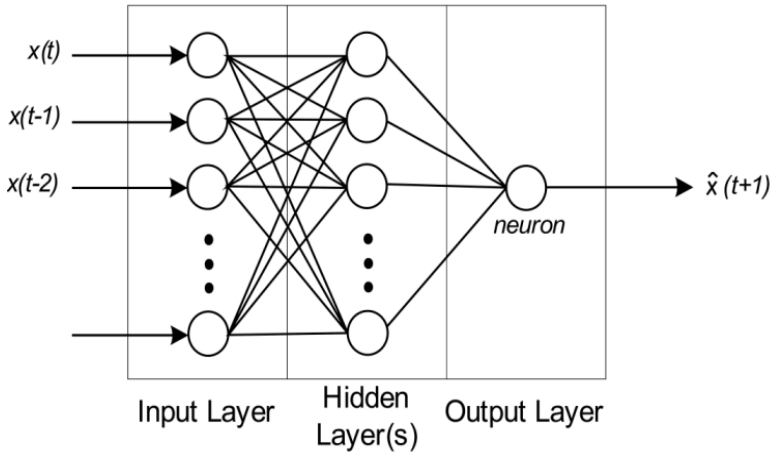

Figure-1: ANN-based time series prediction (Akhlaghinia, 2010)

Connection to each neuron to another neuron for times series prediction is shown in Figure 1. In NN back propagation a set of inputs $(x_1, x_2, \cdots x_i)$ are correlated to a set of outputs $(y_1, y_2, \cdots y_i)$. The input is iteratively multiplied by the weight. Weighted inputs to each upper layer unit are summed up as shown in Eqn.(1):

$$y_i = f\left(w_o\left\{w_h x_i + \phi_h\right\} + \phi_o\right) \quad (1)$$

where $w_o =$ output weight, $w_h =$ hidden layer, $\phi_o =$ output bias, $\phi_h =$ hidden layer bias and $f(.) =$ sigmoid activation function. However, activation functions could be threshold, piece-wise linear and Gaussian.

In the implementation of the neural network, the objective function is to minimize the error function such as the Sum of Square Error (SSE) expressed in Eqn. (2):

$$E = 0.5\sum_{i=1}^{N}\left(t_i - y_i\right)^T\left(t_i - y_i\right) \quad (2)$$

where $t_i =$ target output for pattern i

The gradient descent is used to adjust the inter-neuron weights. If the fan-in weight to a neuron is represented by weight w, then the update in the k[th] epoch is defined by Eqn. (3):

$$\Delta w_k = -\eta \nabla E\left(w\right)\Big| w = w(t) + \alpha \Delta w_{k-1} \quad (3)$$

where $\eta =$ learning rate, which controls the step size of each iteration, $\alpha =$ momentum factor.

The gradient descent will be modified with the Levenberg-Marquardt algorithm to quicken the convergence of the neural network algorithm.

The block diagram of an artificial neural network-based spectrum prediction process is shown in Figure 2.

e-ISSN: 2582-5208
International Research Journal of Modernization in Engineering Technology and Science
Volume:02/Issue:09/September-2020 Impact Factor- 5.354 www.irjmets.com

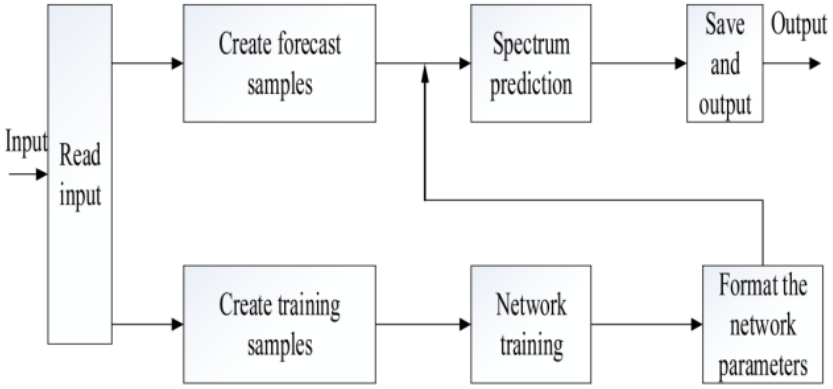

Figure-2: Block of the process of artificial neural network-based spectrum prediction (Hou et al., 2017)

This article investigated the use of Artificial Neural Network in the prediction of the average power spectral densities of GSM 900 band reverse link 925 - 960 MHz in a selected location in Ilorin (8.511^0N, 4.594^0E). In section 2, the ANN configuration is described. Section 3 presents a description of the software and machine configurations used in the study. The results obtained are reported and discussed in section 4.

II. MATERIALS AND METHOD

A. Spectrum Occupancy Data Collection

- Measurement Set-Up

The set up of the measurement system is as shown in Figure 3. The core aspect of the set up is the energy detector, which in this case I the BK PRECISION 2640. The specifications of the energy detection are shown in Table 1.

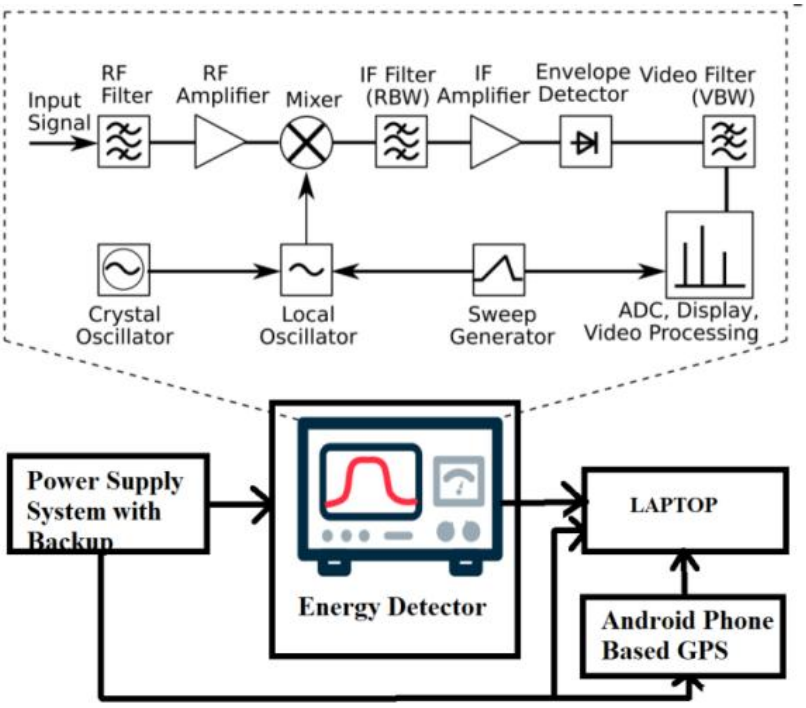

Figure-3: Spectrum data collection set up

The coordinates of the location of measurement were determined using the Android phone-based Global Positioning System (GPS).

Table-3: Selected specifications of the BK PRECISION 2640 field strength analyser

e-ISSN: 2582-5208
International Research Journal of Modernization in Engineering Technology and Science
Volume:02/Issue:09/September-2020 Impact Factor- 5.354 www.irjmets.com

Parameter	Value
Frequency range	100 kHz to 2.0 GHz
Resolution	3.125 Hz
Resolution bandwidth	Variable
Input impedance	50 Ω
Sweep time	Min. 500 ms
Measurement amplitude range	-45 dBm to -110 dBm
Average noise level	-110 dBm max
Input sensitivity	@35 MHz -2,000 MHz: 150 mVrms
Frequency selection mode	Centre, Start/Stop, Span
Reference level accuracy	±3.0dB @ < 600 kHz; ±2.0dB @ ≥ 600 kHz
Log scale	0.2 dB/div minimum in 0.25dB span

Spectrum data, in power spectral densities (dBm), were collected over two weeks using energy detection technique and sort in the form shown in Eqn. (4). The energy detection method is simple and does not require prior knowledge of the measurement environment. The electronic circuit blocks of a typical energy detector are shown in the blown-up section of Figure 3.

$$Y=\begin{bmatrix} p(t_1,f_1) & p(t_1,f_2)\cdots P(t_1,f_j) \\ \vdots & \vdots \quad \vdots \\ p(t_i,f_1) & p(t_i,f_2)\cdots P(t_i,f_j) \end{bmatrix} \tag{4}$$

where Y represents a "matrix of received" signal power in dBm "at each" frequency and time "point" $y_{i,j}$. In the analysis, it is commonly assumed that the noise and signal are "drawn from a complex Gaussian distribution with zero mean and variance" σ^2. Selected work dealing with spectrum measurement across several continents are highlighted next.

- Data Processing

Average power spectral densities PSD_{avg} were computed both spectrally according to frequency point, doing averaging row-wise and temporally, according to time of data collection, doing averaging column-wise. Spectral evaluation is computed using Eqn.(5) and temporal evaluation is computed using Eqn. (6), resulting in a $(1\times n)$ matrix and a $(n\times 1)$ respectively.

$$PSD_{avg\_spec}=\frac{1}{N_t}\sum_{i=j=1}^{N_f} y_{i,j}=\begin{bmatrix} \overline{y}_{1,j} \\ \overline{y}_{2,j} \\ \vdots \\ \overline{y}_{i,j} \end{bmatrix} \tag{5}$$

$$PSD_{avg\_temp}=\frac{1}{N_f}\left[\sum_{i=j=1}^{N_t} y_{1,j},\sum_{i=2,j=1}^{N_t} y_{2,j},\cdots\sum_{i=j=1}^{N_t} y_{i,j}\right]=\left[\overline{y}_{1,j},\overline{y}_{2,j},\cdots\overline{y}_{i,j}\right] \tag{6}$$

e-ISSN: 2582-5208
International Research Journal of Modernization in Engineering Technology and Science
Volume:02/Issue:09/September-2020 Impact Factor- 5.354 www.irjmets.com

where N_f and N_t are the number of frequency point and the number of samples measured in time respectively.

To obtain the final output, the average of the measured power spectral densities in dBm was obtained as shown in Figure 4.

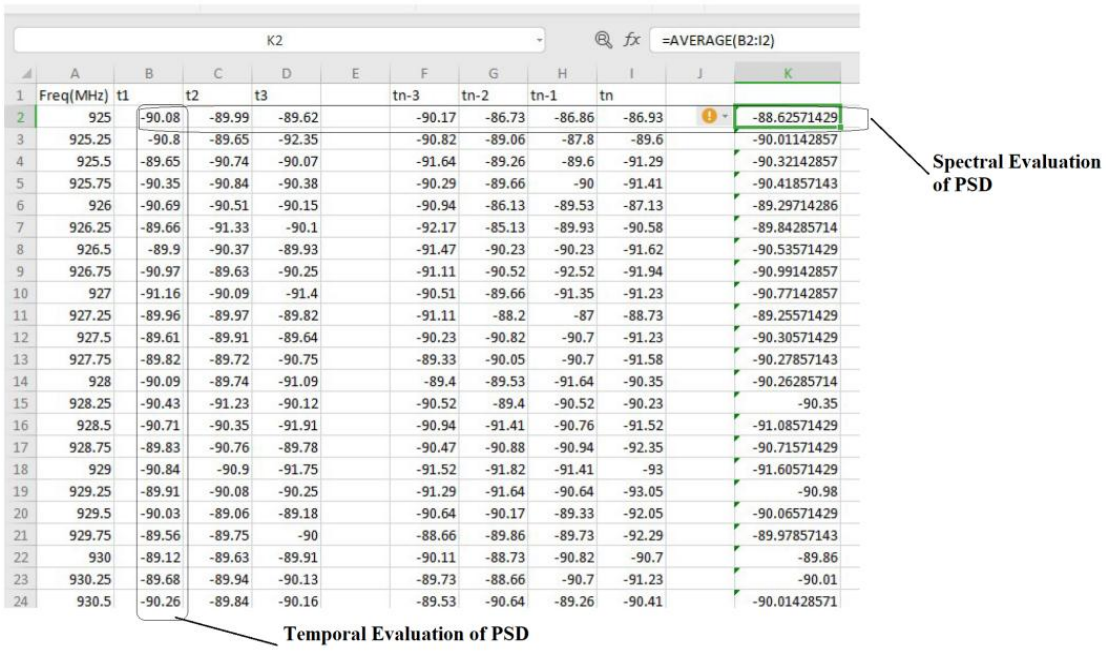

	A	B	C	D	E	F	G	H	I	J	K
1	Freq(MHz)	t1	t2	t3		tn-3	tn-2	tn-1	tn		
2	925	-90.08	-89.99	-89.62		-90.17	-86.73	-86.86	-86.93		-88.62571429
3	925.25	-90.8	-89.65	-92.35		-90.82	-89.06	-87.8	-89.6		-90.01142857
4	925.5	-89.65	-90.74	-90.07		-91.64	-89.26	-89.6	-91.29		-90.32142857
5	925.75	-90.35	-90.84	-90.38		-90.29	-89.66	-90	-91.41		-90.41857143
6	926	-90.69	-90.51	-90.15		-90.94	-86.13	-89.53	-87.13		-89.29714286
7	926.25	-89.66	-91.33	-90.1		-92.17	-85.13	-89.93	-90.58		-89.84285714
8	926.5	-89.9	-90.37	-89.93		-91.47	-90.23	-90.23	-91.62		-90.53571429
9	926.75	-90.97	-89.63	-90.25		-91.11	-90.52	-92.52	-91.94		-90.99142857
10	927	-91.16	-90.09	-91.4		-90.51	-89.66	-91.35	-91.23		-90.77142857
11	927.25	-89.96	-89.97	-89.82		-91.11	-88.2	-87	-88.73		-89.25571429
12	927.5	-89.61	-89.91	-89.64		-90.23	-90.82	-90.7	-91.23		-90.30571429
13	927.75	-89.82	-89.72	-90.75		-89.33	-90.05	-90.7	-91.58		-90.27857143
14	928	-90.09	-89.74	-91.09		-89.4	-89.53	-91.64	-90.35		-90.26285714
15	928.25	-90.43	-91.23	-90.12		-90.52	-89.4	-90.52	-90.23		-90.35
16	928.5	-90.71	-90.35	-91.91		-90.94	-91.41	-90.76	-91.52		-91.08571429
17	928.75	-89.83	-90.76	-89.78		-90.47	-90.88	-90.94	-92.35		-90.71571429
18	929	-90.84	-90.9	-91.75		-91.52	-91.82	-91.41	-93		-91.60571429
19	929.25	-89.91	-90.08	-90.25		-91.29	-91.64	-90.64	-93.05		-90.98
20	929.5	-90.03	-89.06	-89.18		-90.64	-90.17	-89.33	-92.05		-90.06571429
21	929.75	-89.56	-89.75	-90		-88.66	-89.86	-89.73	-92.29		-89.97857143
22	930	-89.12	-89.63	-89.91		-90.11	-88.73	-90.82	-90.7		-89.86
23	930.25	-89.68	-89.94	-90.13		-89.73	-88.66	-90.7	-91.23		-90.01
24	930.5	-90.26	-89.84	-90.16		-89.53	-90.64	-89.26	-90.41		-90.01428571

Figure-4: A screenshot of how the average power spectral densities were obtained.

B. Experiment setup

- System configuration and fitness function

The ANN prediction models used in this research are implemented in MATLAB R2018a on a computer with the following configuration: Intel Core i5, CPU 2.88 GHz, RAM 8 GB, 64-bit operating system. All experiments are conducted on the specified machine. The number of hidden neurons used is 10 and the number of delays is 2. The number of the output layer is 1.

III. RESULTS AND DISCUSSION

In this section, the results obtained are reported. The accuracy of ANN to power spectral density prediction are also shown.

A. Average Power Spectral Density - Based on Frequency Point

Figure 5 shows the average power spectral density evaluated based on frequency points $PSD_{avg-spec}$. It will be observed that the highest power spectral density was obtained at frequency 937.5 MHz with a value corresponding to -57 dBm. Others of fairly strong signal points were observed to be around -76 to -74 dBm.

e-ISSN: 2582-5208
International Research Journal of Modernization in Engineering Technology and Science
Volume:02/Issue:09/September-2020 Impact Factor- 5.354 www.irjmets.com

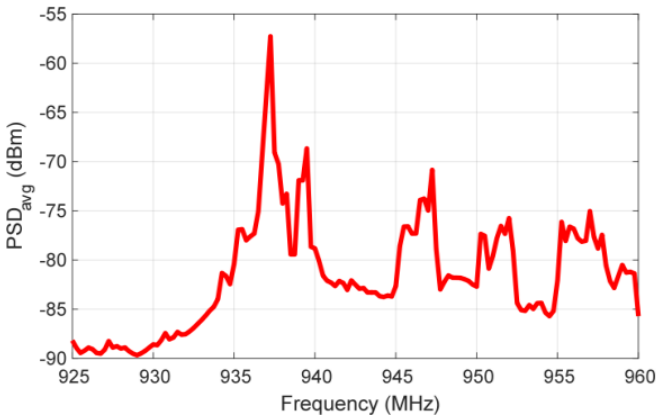

Figure-5: Plot of $PSD_{avg-spec}$ vs GSM 900 RL frequencies

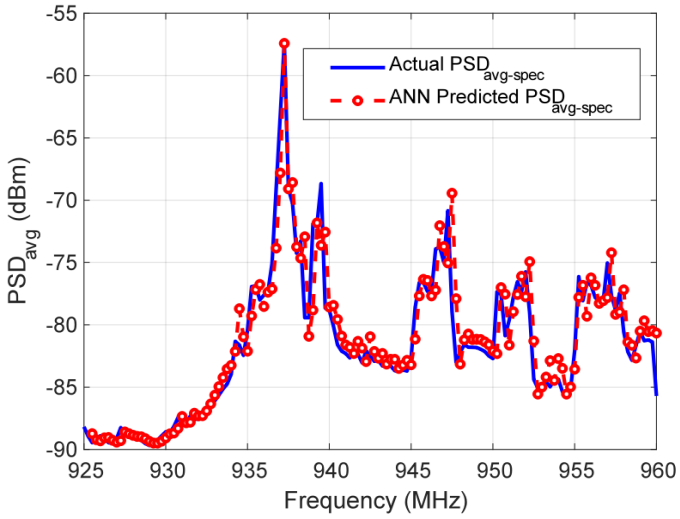

Figure-6: Plot showing the comparison of $PSD_{avg-spec}$ and the predicated one

Figure 6 shows the application of the ANN to the prediction of $PSD_{avg-spec}$ using different sample partitions. The 70-15-15 partition reported the lowest MSE both for training and testing as presented in Tables 2 and 3 respectively.

Table-2: Training MSE with various training, validation and testing ratio

Partition	Mean Square Error		
	Worst	Average	Best
70-15-15	5.6788	3.8291	3.5297
80-10-10	8.9809	4.6465	4.3480
70-20-10	7.1285	3.4944	2.6805

Table-3: Testing MSE with various training, validation and testing ratio

e-ISSN: 2582-5208
International Research Journal of Modernization in Engineering Technology and Science
Volume:02/Issue:09/September-2020 Impact Factor- 5.354 www.irjmets.com

Partition	Mean Square Error		
	Worst	Average	Best
70-15-15	5.0354	3.0724	2.6187
80-10-10	10.9701	3.6205	3.3126
70-20-10	6.2102	5.3411	2.0018

B. Average Power Spectral Density - Based on Time

A plot of the raw data collected is shown in Figure 7. Owing to the noisy nature of the data as shown in the plot, a moving average filter was used to smoothen the waveform. The smoothened plot $PSD_{avg-spec}$ is shown in Figure 8.

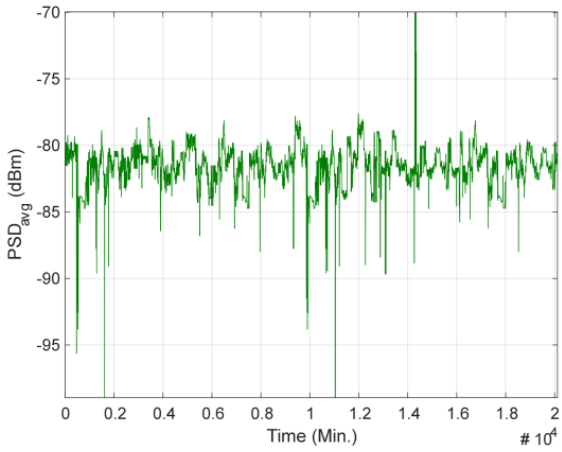

Figure-7: Plot average PSD vs Time

Owing to the noisy nature of the result, a moving average filter was used to smoothen waveform and what was obtained is shown in Figure.

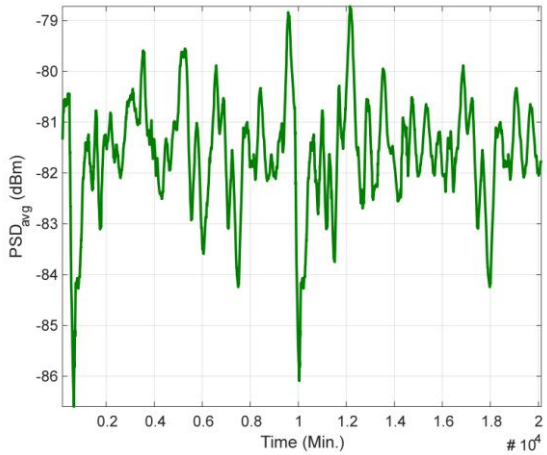

Figure-8: Plot of PSD_{avg_temp} vs time with moving average filter applied

The most accurate sample partition of 70-15-15 was used in predicting the smoothen data and the response and error histogram are shown in Figures 9 and 10 respectively.

e-ISSN: 2582-5208
International Research Journal of Modernization in Engineering Technology and Science
Volume:02/Issue:09/September-2020 Impact Factor- 5.354 www.irjmets.com

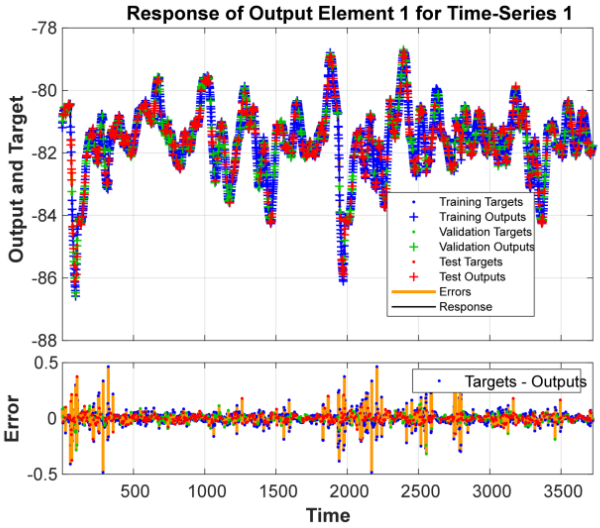

Figure-9: Plot average ANN response to the smoothen PSD_{avg_temp}

The MSE obtained was 0.0025. From the error histogram, it will be observed that the errors are concentrated around -0.08072 to 0.06147.

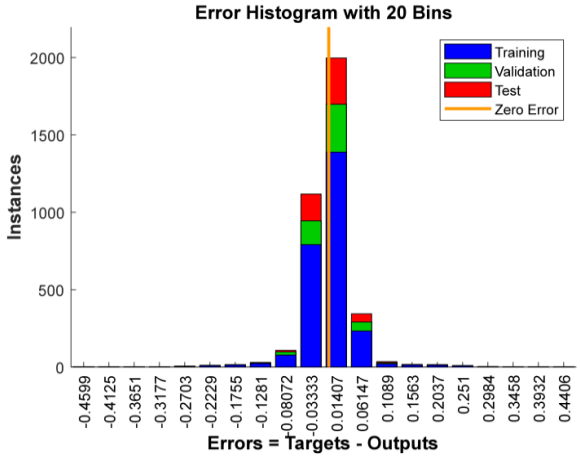

Figure-10: Error histogram from the ANN-based prediction

IV. CONCLUSION

In this research paper, the authors have reported an application of the ANN to the prediction of the average power spectral densities of the GSM 900 band reverse link. Three sample data partition were investigated to determine the most accurate in terms of MSE. The partitions investigated were 70-15-15, 80-10-10 and 70-20-10 in percentages.

The preliminary results obtained for average power spectral densities based on frequency point averaging showed that the 70-15-15 sample data partition gave the best performance. The MSE for this, based on the error between the input data and the predicted data was 3.9090. this partition was used to predict the power spectral density samples of the entire link consisting of 3762 sample points.

After a moving average based filtration to remove the noise from the sample and training using the neural network, the MSE obtained was 0.0025, indicating good prediction.

In the future, we intend to develop a spectrum decision framework to ensure that a secondary user can use predicted vacant spectrum opportunistically. Also, further research will seek to assess the spectrum occupancy duration of the link under consideration. More cellular links will need to be evaluated predictively and analytically.

V. REFERENCES

[1] Bai, S., Zhou, X., & Xu, F. (2015, August). Spectrum prediction based on improved-back-propagation neural networks. In 2015 11th International Conference on Natural Computation (ICNC) (pp. 1006-1011). IEEE.

[2] Bütün, İ., Talay, A. Ç., Altilar, D. T., Khalid, M., & Sankar, R. (2010, April). Impact of mobility prediction on the performance of cognitive radio networks. In 2010 Wireless Telecommunications Symposium (WTS) (pp. 1-5). IEEE.

[3] Jacob, J., Jose, B. R., & Mathew, J. (2014, September). Spectrum prediction in cognitive radio networks: A bayesian approach. In 2014 Eighth International Conference on Next Generation Mobile Apps, Services and Technologies (pp. 203-208). IEEE.

[4] Li, Y., Dong, Y. N., Zhang, H., Zhao, H. T., Shi, H. X., & Zhao, X. X. (2010, June). Spectrum usage prediction based on high-order Markov model for cognitive radio networks. In 2010 10th IEEE International Conference on Computer and Information Technology (pp. 2784-2788). IEEE.

[5] Safari, N., Chung, C. Y., & Price, G. C. D. (2017). Novel multi-step short-term wind power prediction framework based on chaotic time series analysis and singular spectrum analysis. IEEE Transactions on Power Systems, 33(1), 590-601.

[6] Supraja, P., & Pitchai, R. (2019). Spectrum prediction in cognitive radio with hybrid optimized neural network. Mobile Networks and Applications, 24(2), 357-364.

[7] Su, J., & Wu, W. (2009, September). Wireless spectrum prediction model based on time series analysis method. In Proceedings of the 2009 ACM workshop on Cognitive radio networks (pp. 61-66).

[8] Tumuluru, V. K., Wang, P., & Niyato, D. (2010, May). A neural network based spectrum prediction scheme for cognitive radio. In 2010 IEEE International Conference on Communications (pp. 1-5). IEEE.

[9] Xing, X., Jing, T., Huo, Y., Li, H., & Cheng, X. (2013b). Channel quality prediction based on Bayesian inference in cognitive radio networks. In 2013 Proceedings IEEE INFOCOM (pp. 1465-1473). IEEE.

[10] Xing, X., Jing, T., Cheng, W., Huo, Y., & Cheng, X. (2013a). Spectrum prediction in cognitive radio networks. IEEE Wireless Communications, 20(2), 90-96.

[11] Yang, J., & Zhao, H. (2015). Enhanced throughput of cognitive radio networks by imperfect spectrum prediction. IEEE Communications Letters, 19(10), 1738-1741.

[12] Zhang, T., Wang, J., Liu, Q., Zhou, J., Dai, J., Han, X., ... & Xu, K. (2019). Efficient spectrum prediction and inverse design for plasmonic waveguide systems based on artificial neural networks. Photonics Research, 7(3), 368-380.

[13] Zhao, Y., Hong, Z., Wang, G., & Huang, J. (2016, August). High-order hidden bivariate Markov model: A novel approach on spectrum prediction. In 2016 25th International Conference on Computer Communication and Networks (ICCCN) (pp. 1-7). IEEE.